J. Fluid Mech. (1999), *vol.* 399, *pp.* 319–333. Printed in the United Kingdom

A new approach to high-order Boussinesq models

By Y. AGNON[1], P. A. MADSEN[2] AND H. A. SCHÄFFER[3]

[1] Civil Engineering, Technion, Haifa 32000, Israel

[2] Department of Mathematical, Modelling Technical University of Denmark, 2800 Lyngby, Denmark

[3] Danish Hydraulic Institute, Agern Alle 5, 2970 Hørsholm, Denmark

(Received 10 July 1998 and in revised form 2 July 1999)

An infinite-order, Boussinesq-type differential equation for wave shoaling over variable bathymetry is derived. Defining three scaling parameters – nonlinearity, the dispersion parameter, and the bottom slope – the system is truncated to a finite order. Using Padé approximants the order in the dispersion parameter is effectively doubled. A derivation is made systematic by separately solving the Laplace equation in the undisturbed fluid domain and then addressing the nonlinear free-surface conditions. We show that the nonlinear interactions are faithfully captured. The shoaling and dispersion components are time independent.

1. Introduction

Boussinesq-type equations have been widely studied in recent years. The introduction of Padé approximants greatly improves the dispersion and shoaling characteristics of these equations, making them an attractive tool for general coastal applications. A review of the subject is given by Madsen & Schäffer (1998, referred to as MS in the following). The methods used most often for deriving high-order Boussinesq equations are based on two techniques: one is the choice of appropriate velocity variables which improves the dispersion characteristics of the resulting equation, and the other is enhancement of the equations by applying appropriate linear operators to the continuity equation and the momentum equation. In MS the two methods were combined leading to an improved dispersion relation. The variables used are normally a velocity variable (the velocity at some fraction of the depth or the mean velocity) and the free-surface elevation. This choice leads to a time-dependent system in which dispersion, nonlinearity and shoaling are all coupled. In water of intermediate depth, the highest order terms are required for representation of dispersion and shoaling. This is successfully achieved by using Padé approximants. However, in previous studies there appears to be some trade off among the performance regarding nonlinearity, shoaling and dispersion in the different sets of equations. Our primary goal is to present an approach which performs well in all three respects.

The present approach is based on decoupling the problem into two subproblems. One is the linear part of the problem, which involves solving the Laplace equation in the undisturbed fluid domain, and accounts for dispersion and shoaling. The idea of Boussinesq-type equations is to eliminate the vertical coordinate from the problem. In § 2, this is achieved by the use of infinite power series expansions. The kinematic bottom boundary condition then provides a relation between the horizontal and vertical velocities at the still water level. This relation defines the linear dispersion and shoaling characteristics. The equation is then truncated to finite order. Using Padé approximants to order (N,N) gives high accuracy (to order $2N$) for a relatively low effort. This enables us to obtain excellent dispersion and shoaling characteristics. The rationale for obtaining the Padé approximation is presented in a rigorous manner. It is shown that eliminating high-order terms in the PDE is analogous to a Padé approximation. The terms of $O(N+2, N+4, \ldots 2N)$ in the dispersion parameter are eliminated. The time evolution which contains the nonlinear part of the problem is addressed in § 3, using a Taylor series of order m. Typically the order m required to keep an overall prescribed accuracy level does not exceed N.

The full accuracy of the dispersion and shoaling, attained in the linear part of the problem, is carried over to the nonlinear interaction. This is due to the decoupling of the linear and the nonlinear parts of the problem.

Section 4 presents an analysis of the nonlinear performance of the model by examining its second-order superharmonic and subharmonic transfer functions, as well as the third-harmonic, nonlinear dispersion and side-band instability. Conclusions are given in § 5.

In the Appendix, the exact shoaling gradient, which was derived by Madsen & Sørensen (1992) using energy flux conservation, is derived directly from the fully dispersive shoaling equation, in the same way that the approximate shoaling gradient is found for the Boussinesq equations.

2. Eliminating the vertical coordinate

2.1. *An infinite series solution of the Laplace equation on variable depth*

The equations governing the irrotational flow of an incompressible inviscid fluid with a free surface are

$$\nabla^2\phi + \phi_{zz} = 0, \tag{1}$$

$$\eta_t + \nabla\phi \cdot \nabla\eta - \phi_z = 0, \qquad z = \eta, \tag{2}$$

$$\phi_t + \tfrac{1}{2}(\nabla\phi)^2 + \tfrac{1}{2}\phi_z^2 + g\eta = 0, \qquad z = \eta, \tag{3}$$

$$\phi_z + \nabla\phi \cdot \nabla h = 0, \qquad z = -h, \tag{4}$$

where ϕ is the velocity potential, h the water depth, and η the surface elevation. The origin is on the mean free surface and z is positive upwards. The horizontal gradient operator relates ϕ to the horizontal velocity, $\boldsymbol{u}$:

$$\nabla = \left(\frac{\partial}{\partial x}, \frac{\partial}{\partial y}\right), \qquad \boldsymbol{u} = (u, v) = \nabla\phi, \qquad w = \phi_z. \tag{5}$$

One of the main ideas in Boussinesq-type theories is to reduce the three-dimensional description to a two-dimensional one. The first step towards such a reduction is to apply separation of variables and to introduce an expansion of the velocity potential as a power series in the vertical coordinate:

$$\phi(\boldsymbol{x}, z, t) = \sum_{n=0}^{\infty} z^n \phi_n(\boldsymbol{x}, t) \tag{6}$$

By substituting this expansion into (1) we find

$$\phi(\boldsymbol{x}, z, t) = \sum_{n=0}^{\infty}(-1)^n \left(\frac{z^{2n}}{(2n!)}\nabla^{2n}\phi_0 + \frac{z^{2n+1}}{(2n+1)!}\nabla^{2n}\phi_1 \right) \tag{7}$$

which is a series solution with only two unknown functions ϕ_0 and ϕ_1. Note that the velocities at the still water level are given by

$$\boldsymbol{u}_0 = \nabla\phi_0, \qquad w_0 = \phi_1. \tag{8}$$

By the use of (7) and (8) the bottom boundary condition (4) can be expressed as

$$L_c\{w_0\} + L_s \cdot \{\boldsymbol{u}_0\} + \nabla h \cdot \left(L_c\{\boldsymbol{u}_0\} + L_s\{w_0\}\right) = 0 \tag{9}$$

with

$$L_c = \sum_{n=0}^{\infty}(-1)^n \frac{h^{2n}}{(2n)!}\nabla^{2n}, \qquad L_s = \sum_{n=0}^{\infty}(-1)^n \frac{h^{2n+1}}{(2n+1)!}\nabla^{2n+1} \tag{10}$$

where ∇ is the gradient operator when applied to a scalar, and the divergence when applied to a vector. This equation was given by MS, and it defines a general relation between $\boldsymbol{u}_0$ and w_0 which is of infinite order in $h\nabla$. It involves only h and its gradient, but no higher derivatives of it. The series are convergent if ϕ_0 has a Fourier transform, since they correspond to the analytic functions $\sinh kh$ and $\cosh kh$ where ik is the Fourier symbol of ∇. In the next section (9) is approximated at a finite order in the dispersion parameter using Padé approximants. This procedure introduces higher-order terms in the bottom slope, which are consequently truncated.

Following Rayleigh (1876), we may use the symbolic notation of Taylor series operators by which (10) can be given in the compact form

$$L_c = \mathrm{Cos}\,(h\nabla), \qquad L_s = \mathrm{Sin}\,(h\nabla). \tag{11}$$

Note that h and ∇ do not commute, so the powers in (11) are $h^n\nabla^n$ and not $(h\nabla)^n$. It is worth noting that assuming a horizontal bottom ($\nabla h = 0$), (9) may be written in the form

$$w_0 = \mathrm{Tan}\,(h\,\nabla)\,\boldsymbol{u}_0 \tag{12}$$

with Tan defined in analogy to Sin and Cos. In the Appendix (9) is solved with the linearized surface boundary conditions to provide the exact linear dispersion relation and the linear shoaling gradient.

In linear theory

$$\nabla w_0 = -\frac{1}{g}\boldsymbol{u}_{0tt}. \tag{13}$$

Eliminating w_0 between the last two equations gives an evolution equation for $\boldsymbol{u}_0$ from which the linear dispersion relation ($c^2 = \omega^2/k^2 = gh \tanh kh/kh$) is immediately obtained. Here ω is the wave's angular frequency and k is its wavenumber.

2.2. *Approximate solutions of the Laplace equation*

Our goal is to approximate (9) by a finite-order equation. This will correspond to approximating the dispersion relation to a finite order in the dispersion parameter $\mu = k_* h_*$, where k_* is a characteristic wavenumber and h_* a characteristic depth. The shoaling parameter is the characteristic bottom slope $|\nabla h|$. Classical Boussinesq theory is based on Taylor expanding the Tan operator, or $\tanh kh$ to $O(kh)^3$. Even high-order Taylor expansions diverge beyond $kh = \pi/2$ due to a singularity (on the imaginary axis) of the function $\tanh kh$. It is preferable to employ Padé approximants of $\tanh kh/kh$ (in terms of kh). The order in kh of a Padé (N, N) expansion (which involves N^{th} derivatives) is $2N$.

A simple truncation of the Taylor expansion of (9) would lead to

$$\left(1 - \tfrac{1}{2}h^2\nabla^2 + \tfrac{1}{24}h^4\nabla^4\right)w_0 + \left(h\nabla - \tfrac{1}{6}h^3\nabla^3 + \tfrac{1}{120}h^5\nabla^5\right)\cdot \boldsymbol{u}_0 \\ +\nabla h \cdot \left[\left(h\nabla - \tfrac{1}{6}h^3\nabla^3 + \tfrac{1}{120}h^5\nabla^5\right)w_0 + \left(1 - \tfrac{1}{2}h^2\nabla^2 + \tfrac{1}{24}h^4\nabla^4\right)\boldsymbol{u}_0\right] = 0, \tag{14}$$

with errors of $O(kh)^6$ (note that $\boldsymbol{u}_0$ and w_0 are of the same order). The terms which include ∇h are even smaller. Since the slope parameter is independent of the dispersion parameter, the same order of μ is maintained in the slope terms, neglecting terms that are $O(\mu^6, \mu^6\nabla h)$. Padé approximants allow a much higher (at least double) order of accuracy without increasing the order of the derivatives. More importantly, they converge beyond some of the singularities which make the Taylor series of $\tanh kh$ diverge.

Instead of using the truncated Taylor series, MS applied the technique of successive approximations to obtain an explicit expression for w_0 in terms of $\boldsymbol{u}_0$ and used this to eliminate the vertical velocity from the problem. In the present work we retain w_0 as one of the dependent variables and the relation between $\boldsymbol{u}_0$ and w_0 remains as one of our governing equations. Thus, we can apply the enhancement technique from MS to the linear relation, (9). This is somewhat different from the approach of MS, who applied the enhancement technique to the mass and momentum equations (or equivalently, the free-surface boundary conditions). The advantage of the present approach is that nonlinearity and enhancement are not mixed. Let us start the enhancement with the case of uniform depth. Rather than just truncate (9) at some level, $n = N$, one may first multiply it by an operator of the form

$$A = 1 + a_2 h^2\nabla^2 + a_4 h^4\nabla^4 + \dots\ . \tag{15}$$

One way to determine the operator is to require that all terms of orders $N + 2$, $N + 4, \dots, 2N$ vanish. This apparently gives an equation that is correct to $O(\mu^{2N})$. This gives rise to the familiar Padé (N, N) dispersion relation. For $N = 4$ we find that $(a_2, a_4, a_6, a_8) = (1/18, 1/504, 1/15120, 1/362880)$. The resulting PDE is

$$\left(1 - \tfrac{4}{9}h^2\nabla^2 + \tfrac{1}{63}h^4\nabla^4\right)w_0 + \left(h\nabla - \tfrac{1}{9}h^3\nabla^3 + \tfrac{1}{945}h^5\nabla^5\right)\cdot \boldsymbol{u}_0 = 0 \tag{16}$$

which is correct to μ^8. The procedure shown here is analogous to Padé approximation of the function $\tanh kh = \sinh kh/\cosh kh$. The coefficients obtained coincide with the corresponding Padé coefficients.

For the case of variable depth, the elimination of high-order terms is more involved. When multiplying powers of $h\nabla$, terms involving $\nabla h, (\nabla h)^2, \nabla^2 h$ etc. arise. Since h is variable, ∇ and h do not commute, and their ordering affects the product. In the following we shall neglect terms that are $O((\nabla h)^2, \nabla^2 h)$ which arise in manipulating (9). Thus, the present model, along with other Boussinesq-type models, is only valid in situations in which the mild slope equation applies. It does not reproduce the reflected wave field when high-order bottom variation terms are important (cf. Agnon 1999 for an analysis of the importance of high derivatives of the bottom variation). The relevant terms can be incorporated in the model.

While the application of the operator (15) was sufficient for constant depth, variable depth calls for an operator including odd powers of $h\nabla$. Thus, applying $A + B\nabla h$

instead of A to (9), where

$$B = b_1 h \nabla + b_3 h^3 \nabla^3 + \ldots, \tag{17}$$

it is possible to eliminate high-order mild-slope terms with an appropriate choice of the coefficients $b_1, b_2, \ldots$ just as the higher-order constant-depth terms were eliminated above by adjusting the coefficients $a_1, a_2, \ldots$. The shoaling characteristics produced by this approach are unfortunately not very good. The reason is that the error in the dispersion relation affects the shoaling by introducing an error in k_x (which is reproduced well only for smaller kh than the values of kh for which the dispersion approximation works well). k_x appears in the usual analysis of the shoaling characteristics of a monochromatic wave of the form $\eta = A(x) \exp [\mathrm{i}(\omega t - \int k \, \mathrm{d}x)]$, where A and k are slowly varying functions of x, see e.g. MS and the Appendix.

An alternative approach, which solves this problem, is to optimize the coefficients $b_1, b_2, \ldots$ to obtain minimum errors in the shoaling characteristics for a certain range of wavenumbers. The technique is to determine the linear shoaling gradient from (9) multiplied by $A + B\nabla h$ together with the linear surface conditions, similarly to the procedure used by MS. While the constant-depth terms are still correct to $O(\mu^8)$, the mild-slope terms are formally in error at $O(|\nabla h| \, \mu^6)$. This truncation leaves us with two coefficients which can be adjusted for optimal shoaling. Such a procedure was followed by MS and we will show how their results can be used in the present work.

The exact shoaling gradient for Stokes waves, which serves as a reference, was derived by Madsen & Sørensen (1992) from energy flux considerations. In the Appendix we derive the same exact shoaling gradient directly from (9) in the same way that Madsen & Sørensen derived the shoaling gradient for Boussinesq-type equations. This approach unifies the analysis.

Since the linear part of the present model is equivalent to the linear part of MS we shall just relate the results of MS to the present formulation. First of all, we note that w_0 may be expressed in terms of the depth-averaged horizontal velocity in the undisturbed fluid domain, $\boldsymbol{U}_0$:

$$w_0 = -\nabla \cdot (h\boldsymbol{U}_0) \qquad \boldsymbol{U}_0 = \frac{1}{h} \int_{-h}^{0} \boldsymbol{u} \, \mathrm{d}z. \tag{18}$$

Substituting the linearized equation $\boldsymbol{u}_{0t} = -\boldsymbol{g}\nabla\eta$ in (4.11b) of MS and integrating the result with respect to time yields (for the case of Padé (4,4) dispersion)

$$\begin{aligned} &-(1 - \tfrac{4}{9} h^2 \nabla^2 + \tfrac{1}{63} h^4 \nabla^4)\boldsymbol{U}_0 + (1 - \tfrac{1}{9} h^2 \nabla^2 + \tfrac{1}{945} h^4 \nabla^4)\boldsymbol{u}_0 \\ &\quad +\nabla h\big[((1+2\alpha_2)h\nabla - (\beta_2 + \tfrac{1}{27} + \tfrac{2}{3}\alpha_2)h^3\nabla^3) \cdot \boldsymbol{U}_0 + (-2\alpha_2 h\nabla + \beta_2 h^3\nabla^3) \cdot \boldsymbol{u}_0\big] = 0. \end{aligned} \tag{19}$$

Multiplying this equation by h and taking its horizontal gradient, it can be written (in the mild-slope approximation) in the form

$$\begin{aligned} &(1 - \tfrac{4}{9} h^2 \nabla^2 + \tfrac{1}{63} h^4 \nabla^4)w_0 + (h\nabla - \tfrac{1}{9} h^3 \nabla^3 + \tfrac{1}{945} h^5 \nabla^5) \cdot \boldsymbol{u}_0 \\ &\quad + \nabla h \cdot \big[(-(1+2\alpha_2)h\nabla + (\beta_2 + \tfrac{1}{27} + \tfrac{2}{3}\alpha_2)h^3\nabla^3)w_0 \\ &\quad + (1 - (\tfrac{3}{9} + 2\alpha_2)h^2\nabla^2 + (\tfrac{5}{945} + \beta_2)h^4\nabla^4)\boldsymbol{u}_0\big] = 0. \end{aligned} \tag{20}$$

For the bottom-slope terms, the resemblance between the $\boldsymbol{U}_0$-term in (19) and the w_0-term in (20) stems from the equivalence (in the mild-slope approximation) between $\nabla(h^{2n+1}\nabla^{2n}\boldsymbol{U}_0)$ and $h^{2n}\nabla^{2n}(\nabla \cdot (h\boldsymbol{U}_0))$, i.e. the transformation of this part of (19) produces no new bottom-slope terms. MS found that the values $(\alpha_2, \beta_2) = (0.146488,$

0.00798359) give a mean-square error in the shoaling gradient of 3.5×10^{-6}, over the range $0 < kh < 6$. The shoaling gradient is defined as the ratio between A_x/A and $-h_x/h$, where A is the slowly varying amplitude of a monochromatic wave.

Now that the relation between w_0 and $\boldsymbol{u}_0$ has been established, we turn to the nonlinear part of the problem, the free-surface boundary conditions, which can be viewed as evolution equations.

3. The nonlinear time-stepping problem

Following Zakharov (1968), Witting (1984) and Dommermuth & Yue (1987), we choose to reformulate the dynamic and kinematic boundary conditions at the free surface by introducing velocity variables and the velocity potential defined directly at the free surface, i.e.

$$\tilde{\boldsymbol{u}} \equiv (\nabla \Phi)_{z=\eta}, \qquad \tilde{w} \equiv (\Phi_z)_{z=\eta}, \tag{21}$$

$$\tilde{\Phi} \equiv \Phi(x, y, \eta, t), \qquad \tilde{\boldsymbol{V}} \equiv \nabla \tilde{\Phi}. \tag{22}$$

Now spatial and temporal differentiation of $\tilde{\Phi}$ involves the chain rule, and we have

$$\nabla \tilde{\Phi} = (\nabla \Phi)_{z=\eta} + \nabla \eta (\Phi_z)_{z=\eta} + \cdots = \tilde{\boldsymbol{u}} + \tilde{w} \nabla \eta + \ldots, \tag{23}$$

$$\tilde{\Phi}_t = (\Phi_t)_{z=\eta} + \eta_t (\Phi_z)_{z=\eta} + \cdots = (\Phi_t)_{z=\eta} + \tilde{w}^2 - \tilde{w} \nabla \eta \cdot \tilde{\boldsymbol{u}} + \ldots, \tag{24}$$

where the time derivative of η has been eliminated by use of (2). After some algebra the dynamic condition (3) can be expressed as

$$\tilde{\Phi}_t + \eta + \frac{\tilde{\boldsymbol{V}} \cdot \tilde{\boldsymbol{V}}}{2} - \frac{\tilde{w}^2}{2} - \frac{\tilde{w}^2}{2} \nabla \eta \cdot \nabla \eta = 0. \tag{25}$$

This is the formulation used by Dommermuth & Yue (1987). As an alternative, we can apply the gradient operator to (25), which transfers the equation into a velocity vector equation used by e.g. Witting (1984),

$$\tilde{\boldsymbol{V}}_t + \nabla \eta + \nabla \left(\frac{\tilde{\boldsymbol{V}} \cdot \tilde{\boldsymbol{V}}}{2} - \frac{\tilde{w}^2}{2} - \frac{\tilde{w}^2}{2} \nabla \eta \cdot \nabla \eta \right) = 0. \tag{26}$$

Finally, the combination of (21) and (2) yields the kinematic condition

$$\eta_t - \tilde{w} + \nabla \eta \cdot \tilde{\boldsymbol{u}} = 0. \tag{27}$$

We note that (26) and (27) express the fully nonlinear time-stepping problem, but to solve the system, a closure between the quantities $\tilde{\boldsymbol{V}}$, $\tilde{\boldsymbol{u}}$, and $\tilde{w}$ is necessary. This closure can be established by the use of (7) and (8), which lead to high-order relations between the velocities at the free surface and the velocities at the still water level. Since the vertical structure of the flow field is approximated by an algebraic function of z, and further, the range of wave steepness $k\eta = O(\epsilon)$ is smaller than the range of kh considered, it is sufficient to include just a few terms in a Taylor expansion about the free surface in the manner used in perturbation theories. For definiteness, we adopt the fourth-order expansion employed by other (4,4) Boussinesq-type models:

$$\tilde{\boldsymbol{u}} = \boldsymbol{u}_0 + \eta \nabla w_0 - \frac{\eta^2}{2} \nabla \nabla \cdot \boldsymbol{u}_0 - \frac{\eta^3}{6} \nabla \nabla^2 w_0 + \frac{\eta^4}{24} \nabla^4 u_0 + O(\epsilon^5), \tag{28}$$

$$\tilde{w} = w_0 - \eta \nabla \cdot \boldsymbol{u}_0 - \frac{\eta^2}{2} \nabla^2 w_0 + \frac{\eta^3}{6} \nabla^2 \nabla \cdot \boldsymbol{u}_0 + \frac{\eta^4}{24} \nabla^4 w_0 + O(\epsilon^5), \tag{29}$$

$$\tilde{\boldsymbol{V}} = \boldsymbol{u}_0 + \nabla\left(\eta w_0 - \frac{\eta^2}{2}\nabla\cdot\boldsymbol{u}_0 - \frac{\eta^3}{6}\nabla^2 w_0 + \frac{\eta^4}{24}\nabla^4 u_0\right) + O(\epsilon^5). \tag{30}$$

When calculating short waves riding over long waves, $k\eta$ becomes large, but so does kh, and both the dispersion and nonlinearity of the model become less faithful.

The system of equations to be solved now consists of (26), (27), (28), (29), (30), and (20), i.e. six coupled equations in six variables (counting vectors as one): the surface elevation, the horizontal gradient of the free-surface velocity potential, the horizontal and vertical velocities at the free surface and at the mean sea level. At each time step, after marching (26) and (27) in time, the system to be solved for $\tilde{\boldsymbol{u}}$, $\boldsymbol{u}_0$, w_0 and $\tilde{w}$ is linear.

4. Evaluation of the nonlinear interaction

Convenient measures of nonlinear interaction over a horizontal bottom are the transfer functions to superharmonics and to subharmonics via triad interaction. Since the only approximation made was in the solution to the Laplace equation, it is easily checked that the only error in the transfer functions in the present model stems from the error in the dispersion relation. For the transfer functions the error will be due to the error in the dispersion of the primary wave and the error in the dispersion of the bound wave, which in the case of a superharmonic, has a higher value of kh and thus a larger error than the primary waves. In the case of a subharmonic, the error is determined by the relative error in the difference frequency, which is again greater than the error for the primary waves. The expressions for the transfer functions in the fully dispersive water wave problem can be found e.g. in Hasselmann (1962).

Figure 1 shows the second-order transfer functions for the present set of equations normalized by the transfer functions for exact dispersion. Figure 1(*a*) shows the accuracy of the second harmonic in a Stokes wave for the present Padé (4,4) model (curve i) compared with the best Padé (4,4) model from MS (their U model). Vast improvement is seen. Figure 1(*b*) shows the accuracy of the superharmonics and the subharmonics for the present model. On the axes are shown the normalized values of the frequencies of the primary waves. The value of 0.4 corresponds to kh exceeding 6.3. The subharmonic of two waves with close wavenumbers (just below the diagonal) is related to the wave setdown. It is driven by the radiation stress and depends on the group velocity. The error in the setdown is related to errors in the group velocity, which are greater than errors in the wave celerity. The subharmonics, and the setdown are related to the wave-induced mean flow. Both the superharmonics and the subharmonics are slightly underestimated by the model. Note the regular form of the curves in figure 1 which attests to the proper balance of the theory.

In a similar way one can find the third harmonic and the amplitude dispersion of a Stokes wave. The equations found in the literature contain trigonometric equivalences in which expressions such as e.g. $\tanh 2kh$ and $\tanh 3kh$ are expressed in terms of $\coth kh$ etc. Thus they are correct only for the Stokes theory. Thus we rederive their full forms from the Zakharov equations, whose coefficients T, $\tilde{T}^{(1)}$ and $\tilde{T}^{(4)}$ are given in the Appendix of Stiassnie & Shemer (1984) (the second sign in their equation (2*a*) should be +). The expression for $\omega^{(2)}$, the Stokes frequency correction, is given by

$$\begin{aligned}\frac{\omega^{(2)}}{a^2} &= \frac{2\pi^2 g}{\omega}T(k,k,k,k)\\ &= \frac{\left(((gk)^2+\omega^4)\,\omega_2/\omega + 2\,(2\,(gk)^2-\omega^2\,\omega_2^2)\right)^2}{16g^2\,\omega\left(4\,\omega^2-\omega_2^2\right)} + \frac{\left(-(gk)^2\,\omega+\omega_2^2\,\omega^3\right)}{4g^2},\end{aligned} \tag{31}$$

where ω and ω_2 are the angular frequencies from the approximate Padé linear

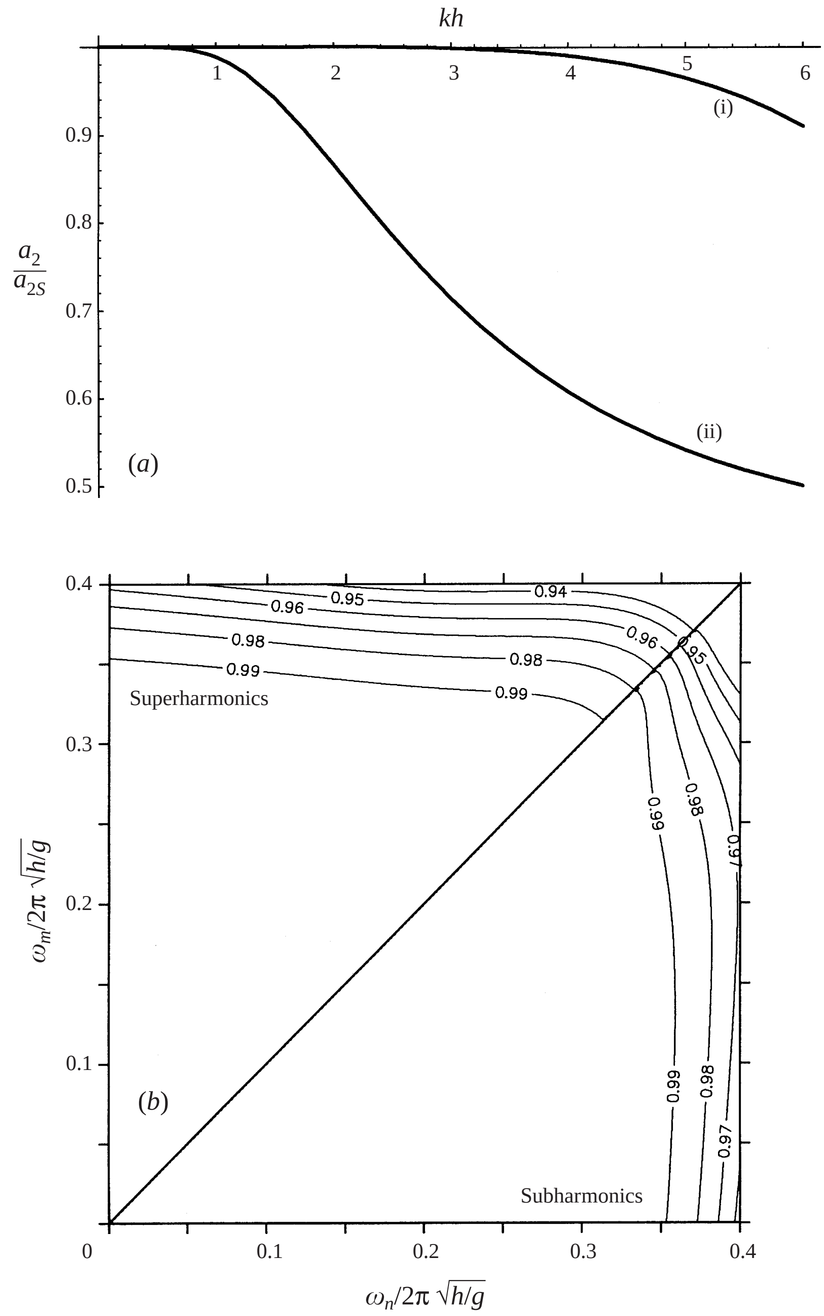

FIGURE 1. (*a*) The relative amplitude of the second harmonic, a_2/a_{2S}, where a_2 is given by the Boussinesq-type (Padé (4,4)) model and a_{2S} is the Stokes theory value. Curve (i) present model; curve (ii) U model (MS). (*b*) The relative (to Stokes theory) second-order transfer function. Superharmonic values shown above the diagonal, subharmonics below the diagonal.

dispersion relation for k and $2k$, respectively. Here a is the wave amplitude. The reduced form of this equation, valid for the exact dispersion relation, is given by

$$\frac{\omega_S^{(2)}}{a^2} = \frac{k^3\left(9 - 10\tanh(kh)^2 + 9\tanh(kh)^4\right)}{16\tanh(kh)^3\sqrt{k\;\tanh(kh)/g}} \tag{32}$$

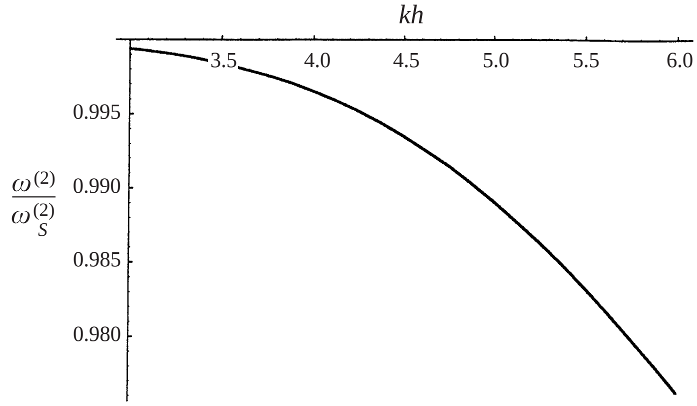

FIGURE 2. The relative value of the Stokes frequency correction, $\omega^{(2)}/\omega_S^{(2)}$, Padé (4,4).

where S stands for Stokes theory (e.g. Whitham 1974). The expression for a_3 is very lengthy and is not expanded here. It contains ω, ω_2 and ω_3. In terms of Zakharov's coefficients it is

$$\frac{a_3}{a^3} = 2\pi^2 g\sqrt{\frac{\omega_3}{\omega^3}}\left(\frac{\tilde{T}^{(1)}(3k,k,k,k)}{\omega_3 - 3\omega} + \frac{\tilde{T}^{(4)}(-3k,k,k,k)}{\omega_3 + 3\omega}\right). \tag{33}$$

The reduced form is given by

$$\frac{a_{3S}}{a^3} = \frac{3\,k^2\left(1 + 8\cosh\left(kh\right)^6\right)}{64\,\sinh\left(kh\right)^6} \tag{34}$$

(e.g. Wehausen & Laitone 1960). Figures 2 and 3 show the relative values of $\omega^{(2)}$ and the values of a_3, respectively, for a Padé (4,4) dispersion relation. The good performance of $\omega^{(2)}$ in the range considered was not expected in view of its dependence on ω_2. For higher values of kh the error in $\omega^{(2)}$ becomes positive and indeed grows rapidly. However, in the range for which this model is considered, nonlinear dispersion is faithfully reproduced. The large error in a_3 for large kh is expected , since it depends on ω_3. For kh up to about 3 the agreement with Stokes theory is good.

In considering the side-band instabilities studied by Benjamin & Feir (1967), the determining parameters are $\Omega^{(2)}$, the frequency correction modified by the wave-induced mean flow,

$$\Omega^{(2)} = \omega^{(2)} + \tilde{\omega}^{(2)}, \tag{35}$$

$$\tilde{\omega}^{(2)} = -kU + \frac{\partial \omega}{\partial h} b \tag{36}$$

(where U is the current associated with the induced mean flow potential ϕ_{10} and b is the setdown), and ω_{kk}, the derivative of the group velocity, c_g, with respect to k. We need an expression for ϕ_{10} which is valid for the present model (and does not rely on trigonometric equivalences). Such a solution was derived by Agnon & Mei (1985). It applies for the present model if their $\sigma = \omega^2/g$ is replaced by the Padé approximation to that expression. The homogeneous part of the long-wave equation which governs ϕ_{10} remains unchanged in the present model, since it is exact at the long-wave limit.

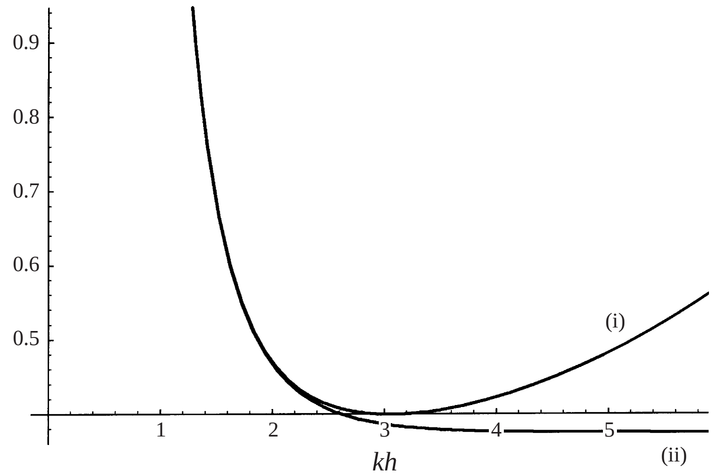

FIGURE 3. The value of the third harmonic amplitude. Curve (i) $a_3/(k^2a^3)$, Padé (4,4); curve (ii) $a_{3S}/(k^2a^3)$.

From Agnon & Mei (1985) we get

$$b = -\frac{1}{g}\phi_{10t} - \frac{g(k^2 - \sigma^2)a^2}{4\omega^2}, \tag{37}$$

$$\phi_{10t} = \frac{a^2 c_g}{4\omega^2(gh - c_g^2)}((g^2k^2 - \omega^4)c_g + 2g^2\omega k), \tag{38}$$

$$U = \phi_{10x} = -\frac{1}{c_g}\phi_{10t}. \tag{39}$$

Figure 4 shows the relative values of ω_{kk} and $\omega^{(2)}$ for a Padé (4,4) dispersion relation; $\tilde{\omega}^{(2)}$ has a small error for $kh < 6$, while for ω_{kk}, good agreement with the exact linear dispersion relation is found only for kh up to about 3. As with the group velocity, the error here is increased by taking an even higher derivative of ω with respect to k. As for $\omega^{(2)}$, the agreement for $\tilde{\omega}^{(2)}$ is better than expected, due to opposite trends in its ingredients. As kh increases, the error again rapidly increases. The onset of the side-band instability is determined by the sign of $\omega_{kk}\Omega^{(2)}$; ω_{kk} is negative and $\Omega^{(2)}$ becomes negative (instability) for $kh > 1.363$ which is also the value for the exact theory. Thus the onset of the side-band instability is accurately modelled. For weakly nonlinear waves, the bandwidth of the instability (divided by the wave amplitude) is $4(\Omega^{(2)}/\omega_{kk})^{1/2}$. From figures 2 and 4 it is clear that in the range considered, the error in this ratio is dominated by the error in ω_{kk}. Thus the former is approximately the inverse of the square root of the latter. Since the approximated ω_{kk} becomes considerably smaller than the exact value, the bandwidth of growing disturbances is increased by more than 50% for $kh = 6$. The maximal growth rate is greater by a similar factor.

In MS the expression for the amplitude of the second and third harmonic was expanded in a power series in kh. Agreement with Stokes theory was attainable up to $O(\mu^4)$. In the present model all the nonlinear quantities agree with Stokes theory to the same order as the dispersion relation does, i.e. to $O(\mu^8)$.

In a shoaling model it is of interest to examine the combined effect of shoaling and nonlinearity. In the standard model for water waves, the nonlinear shoaling

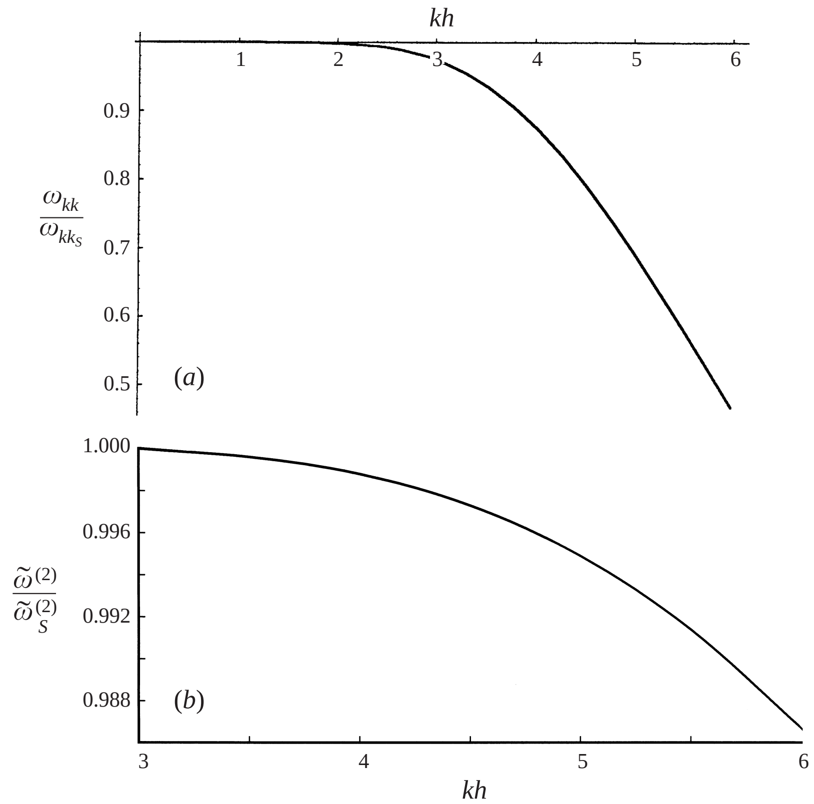

FIGURE 4. (*a*) The relative value of the derivative of c_g, ω_{kk}/ω_{kkS}, Padé (4,4). (*b*) The relative value of the frequency correction due to the wave-induced mean flow, $\tilde{\omega}^{(2)}/\tilde{\omega}_S^{(2)}$, Padé (4,4).

and modulation of wave trains and wave packets can be described by the well-established nonlinear Schrödinger equation (NLS, cf. Benney & Newell 1967; Davey & Stewartson 1974; Djordjevic and Redekopp 1978). We write here the form that applies to wave shoaling in one horizontal dimension:

$$\mathrm{i}\frac{\partial B}{\partial \xi} + \lambda_1 \frac{\partial^2 B}{\partial \tau^2} - \nu_1 |B|^2 B = -\mathrm{i}\mu_1 B, \tag{40}$$

$$\lambda_1 = \omega_{kk}/(2c_g^3), \tag{41}$$

$$\mu_1 = \frac{1}{2c_g}\frac{\mathrm{d}c_g}{\mathrm{d}\xi}, \tag{42}$$

$$\nu_1 = 4\omega^{(2)}/(c^2 c_g), \tag{43}$$

where B is the complex amplitude of the wave envelope, modified by a phase shift due to the mean flow. We do not discuss the mean flow in detail, and just note that its accuracy is similar to that of the nonlinear interaction. $\xi = \epsilon^2 x$ and $\tau = \epsilon(\int^x (\mathrm{d}x/c_g(\xi)) - t)$ are the multiple scale coordinates.

In the present model, the coefficients are replaced by their approximate values. Examining these approximate coefficients, we can see the fidelity of the model. The shoaling is controlled by the shoaling coefficient μ_1, which is identical to the one of linear shoaling (see the Appendix). MS have shown that the latter is approximated very well in the range $0 < kh < 6$. Terms in the bottom slope that are nonlinear in ϵ might cause concern, most obviously since the higher harmonics have higher waveumbers and are less accurate. These terms do not appear in NLS, neither do they appear in lower-order (triad interaction) shoaling models on a steeper slope (cf. Agnon & Sheremet 1997). Their contribution is higher order, hence their accuracy has a very small influence on the leading-order, free waves. Next, consider the nonlinear interaction. As in the analysis of waves on an even bottom, for the leading-order, free waves, it is governed by $\Omega^{(2)} = \omega^{(2)} + \tilde{\omega}^{(2)}$. We saw in figures 2, 4(b) that it is accurately reproduced. Note that the nonlinear interaction at the leading order is determined by the coefficient T in the Zakharov equation, which is reproduced well, while higher-order (and less important), bound waves, such as a_2 and further, a_3 (which is determined by $\tilde{T}^{(1)}$ and $\tilde{T}^{(4)}$), have greater errors. Finally, the modulation is determined here, again, by the collinear modulation parameter ω_{kk}, which was seen in figure 2(a) to perform well only up to kh of about 3.

We may also write NLS for waves that are modulated in the transverse, y-direction. Benney & Roskes (1969) studied oblique side-band instabilities. These are governed again by $\Omega^{(2)}$ and by a combination of the collinear modulation parameter ω_{kk}, which is negative, and in addition by the transverse modulation parameter c_g/k, which is positive. Thus oblique side-band instabilities can occur also when kh is smaller than 1.363. Since c_g/k is better approximated than ω_{kk} is, the latter remains the limiting factor on the accuracy of the present model. Thus the oblique and the collinear side-band instabilities are modelled with the same accuracy.

NLS is a narrow-band approximation, assuming a small spectral bandwidth. For finite spectral separation, the Zakharov equation can be used (Stiassnie & Shemer 1984). Let us consider side-band instability for a finite-width side band. The accuracy of the interaction kernel T for finite spectral width is represented quite well by $\omega^{(2)}$ (figure 2) for that case as well. At any rate, the limiting factor is again the modulation parameter, which this time is

$$\frac{\omega_- - 2\omega + \omega_+}{K^2} \tag{44}$$

where $\omega_- = \omega(k-K)$ and $\omega_+ = \omega(k+K)$ are the side-band frequencies, and $2K$ is the modulation band width. One option to try to assess the effect of the finite band width on the accuracy of the modulation parameter, is by considering higher-order terms in the spectral width, e.g. ω_{kkk}, which is the coefficient of the next term appearing in the modified Schrödinger equation due to Dysthe. Since the error in ω_{kkk} is very large, this approach would have led us to the erroneous conclusion that the error in the finite band-width case is larger than the error for narrow spectra. Instead we have examined directly the error in the modulation parameter (44) and found that it is in fact smaller than the error for the modulation parameter in the narrow-band case, ω_{kk}. We carried out a similar analysis for the lower-order, (non-resonant) triad interaction. There, again, the modulation parameter is most accurately reproduced at the limit of triad resonance. At that limit it has the value c_g which is reproduced by the model more accurately than ω_{kk} is. Thus the accuracy found for the narrow-band case holds for finite band width as well.

5. Conclusions

A new Boussinesq-type formulation has been presented. The method decouples the solution into two parts. One is the linear part of the system, which accounts for shoaling and dispersive effects. It requires solution of the Laplace equation in a domain which is independent of time. This solution can be found most effectively by enhancing the equation as well as presolving a substantial part of the problem. The second, nonlinear part is the marching in time, using the nonlinear free-surface boundary conditions. By separating the two parts, the accuracy of the linear dispersion is carried in full to the nonlinear part of the system. This would have required a horrendous number of terms if it was to be achieved in the traditional way, i.e. ending up with only two governing equations: one for mass and one for momentum.

Using the velocities at the still water level as variables yields excellent performance in terms of nonlinearity while retaining optimal dispersion characteristics. The nonlinear interaction was evaluated by computing the transfer functions to second-order superharmonics and subharmonics in irregular waves, and the third-harmonic, nonlinear dispersion and side-band instability in regular waves. The same coefficients describe (and place bounds on) the evolution of NLS (and Zakharov equation) models. In the Appendix the exact shoaling model was used for an alternative derivation of the shoaling gradient which is not based on energy flux and does not neglect reflection. It confirms the results of Madsen & Sørensen (1992).

This work was partly financed by the Danish National Research Foundation and partly by the Danish Technical Research Council (STVF grant no. 9801635). Their financial support is greatly appreciated.

Appendix. The exact linear shoaling gradient

In this Appendix we derive the exact linear dispersion relation and the exact linear shoaling gradient on the basis of the combination of the bottom boundary condition and the Laplace solution as given by (9) with (11). Invoking the linearized surface boundary conditions this may be written as a wave equation in terms of the surface elevation

$$\mathrm{Cos}\,(h\nabla)\{\eta_{tt}\} - g\ \mathrm{Sin}\,(h\nabla)\{\nabla\eta\} - \nabla h \cdot (g\ \mathrm{Cos}\,(h\nabla)\{\nabla\eta\} + \mathrm{Sin}\,(h\nabla)\{\eta_{tt}\}) = 0. \tag{A 1}$$

Restricting ourselves to one horizontal dimension, we look for solutions of the form

$$\eta(x,t) = A(x)\mathrm{e}^{\mathrm{i}(\omega t - \int k\,\mathrm{d}x)} \tag{A 2}$$

where A, k, and h are slowly varying functions of x. When evaluating the derivatives of η, only constant-depth terms and mild-slope terms are retained (i.e. only the zeroth and first derivatives of A, k, and h). This leads to

$$\frac{\partial^n\eta}{\partial x^n} = \left((-\mathrm{i}k)^n + n(-\mathrm{i}k)^{n-1}\frac{A_x}{A} - \frac{\mathrm{i}}{2}n(n-1)(-\mathrm{i}k)^{n-2}k_x\right)\eta. \tag{A 3}$$

Looking at the right-hand side of this expression, we notice that the first and second derivative of the first term with respect to $-\mathrm{i}k$ appears in the second and third terms. Let p denote a polynomial (or Taylor series), then this observation leads to

$$p\left(\frac{\partial}{\partial x}\right)\eta = \left(p(-\mathrm{i}k) + p'(-\mathrm{i}k)\frac{A_x}{A} - \frac{\mathrm{i}}{2}p''(-\mathrm{i}k)k_x\right)\eta \tag{A 4}$$

where the prime stands for the derivative. Choosing the polynomial as $(-1)^n h^{2n}/(2n)!\partial^{2n}/\partial x^{2n}$, $n = 0, 1, 2\ldots$, we get

$$\mathrm{Cos}\left(h\frac{\partial}{\partial x}\right)\{\eta_{tt}\} = -\omega^2\left(\cosh(kh) + \mathrm{i}h\sinh(kh)\frac{A_x}{A} + \frac{\mathrm{i}h^2}{2}\cosh(kh)k_x\right)\eta. \tag{A 5}$$

Similarly, the polynomial $(-1)^n h^{2n+1}/(2n+1)!\partial^{2n+2}/\partial x^{2n+2}$, $n = 1, 2\ldots$, yields

$$\mathrm{Sin}\left(h\frac{\partial}{\partial x}\right)\left\{\frac{\partial}{\partial x}\eta\right\} = \left(-k\sinh(kh) - \mathrm{i}\,(\sinh(kh) + kh\cosh(kh))\frac{A_x}{A} \right.$$
$$\left. -\frac{\mathrm{i}h}{2}(2\cosh(kh) + kh\sinh(kh))\,k_x\right)\eta. \quad \text{(A 6)}$$

For the remaining two terms in (A 1), we only need to retain the leading order in the operators and thus it suffices to substitute $-\mathrm{i}k$ for $\partial/\partial x$:

$$h_x\ \mathrm{Cos}\left(h\frac{\partial}{\partial x}\right)\left\{\frac{\partial}{\partial x}\eta\right\} = h_x(-\mathrm{i}k\cosh(kh))\,\eta, \quad \text{(A 7)}$$

$$h_x\ \mathrm{Sin}\left(h\frac{\partial}{\partial x}\right)\{\eta_{tt}\} = -h_x\omega^2(-i\sinh(kh))\,\eta. \quad \text{(A 8)}$$

Substituting (A 5)–(A 8) in the unidirectional version of (A 1) yields, for the real part, the dispersion relation

$$\omega^2 = gk\tanh(kh), \quad \text{(A 9)}$$

and, for the imaginary part, the shoaling equation

$$\frac{A_x}{A}\left(kh + \tfrac{1}{2}\sinh(2kh)\right) + \frac{k_x}{k}\left(kh\cosh^2(kh)\right) + \frac{h_x}{h}(kh) = 0. \quad \text{(A 10)}$$

The final step is to utilize

$$\frac{k_x}{k} = -\frac{G}{1+G}\frac{h_x}{h}, \qquad G \equiv \frac{2kh}{\sinh(2kh)}, \quad \text{(A 11)}$$

which results from the dispersion relation (Madsen & Sørensen 1992, by which (A 10) becomes

$$\frac{A_x}{A} = -\frac{G}{(1+G)^2}\left(1 + \tfrac{1}{2}G(1-\cosh(2kh))\right)\frac{h_x}{h}. \quad \text{(A 12)}$$

This result is identical to the one derived by Madsen & Sørensen (1992) using energy flux considerations and Stokes linear wave theory.

REFERENCES

Agnon, Y. 1999 Linear and nonlinear refraction and Bragg scattering of water waves. *Phys. Rev.* E **59**, 1319–1322.

Agnon, Y. & Mei, C. C. 1985 Slow drift motion of a two-dimensional block in beam seas. *J. Fluid Mech.* **151**, 279–294.

Agnon, Y. & Sheremet, A. 1997 Stochasic nonlinear shoaling of directional spectra. *J. Fluid Mech.* **345**, 79–99.

Benjamin, T. B. & Feir, J. E. 1967 The disintegration of wave trains on deep water. *J. Fluid Mech.* **27**, 417–430.

Benney, D. J. & Newell, A. C. 1967 The propagation of nonlinear wave envelopes. *J. Math. Phys.* **46**, 133–139.

Benney, D. J. & Roskes, G. J. 1969 Wave instabilities. *Stud. Appl. Maths* **48**, 377–385.

Davey, A. & Stewartson, K. 1974 On three-dimensional packets of surface waves. *Proc. R. Soc. Lond.* A **338**, 101–110.

Djordjevic, V. D. & Redekopp, L. G. 1976 On the developments of packets of surface gravity waves moving over an uneven bottom. *Z. Angew. Math. Phys.* **29**, 950–962.

DOMMERMUTH, D. G. & YUE, D. K. P. 1987 A high-order spectral method for the study of nonlinear gravity waves. *J. Fluid Mech.* **184**, 267–288.

HASSELMANN, K. 1962 On the nonlinear energy transfer in a gravity wave spectrum. 1. General theory. *J. Fluid Mech.* **12**, 481–500.

MADSEN, P. A. & SCHÄFFER, H. A. 1988 Higher order Boussinesq-type equations for surface gravity waves – derivation and analysis. *Phil. Trans. R. Soc. Lond.* A **356**, 3123–3184 (referred to herein as MS).

MADSEN, P. A. & SØRENSEN, O. R. 1992 A new form of the Boussinesq equations with improved linear dispersion characteristics. Part 2: A slowly varying bathymetry. *Coastal Engng* **18**, 183–204.

RAYLEIGH, LORD 1876 On waves. *Phil. Mag*. **5**(1), 257–279.

STIASSNIE, M. & SHEMER, L. 1984 On modifications of the Zakharov equation for surface gravity waves. *J. Fluid Mech.* **143**, 47–67.

WEHAUSEN, J. V. & LAITONE, E. 1960 Surface waves. In *Handbuch der Physik*, **IX** (ed. S. Flügge), pp. 446–778. Springer.

WHITHAM, G. B. 1974 *Linear and Nonlinear Waves*. J. Wiley and Sons.

WITTING, J. M. 1984 A unified model for the evolution of nonlinear water waves. *J. Comput. Phys.* **56**, 203–236.

ZAKHAROV, V. E. 1968 Stability of periodic waves of finite amplitude on the surface of a deep fluid. *J. Appl. Mech. Tech. Phys.* **9**, 190–194 (Translation).